

The crystal structure, transport and thermodynamic properties of ThCoGa₄ single crystals

This article has been downloaded from IOPscience. Please scroll down to see the full text article.

2004 J. Phys.: Condens. Matter 16 5427

(<http://iopscience.iop.org/0953-8984/16/30/005>)

View [the table of contents for this issue](#), or go to the [journal homepage](#) for more

Download details:

IP Address: 129.252.86.83

The article was downloaded on 27/05/2010 at 16:13

Please note that [terms and conditions apply](#).

The crystal structure, transport and thermodynamic properties of ThCoGa₄ single crystals

Ryszard Wawryk¹, Julia Stepien-Damm¹, Zygmunt Henkie¹,
Tomasz Cichorek² and Frank Steglich²

¹ W Trzebiatowski Institute of Low Temperature and Structure Research, Polish Academy of Sciences, ulica Okólna 2, 50-950 Wrocław 2, PO Box 1410, Poland

² Max Planck Institute for the Chemical Physics of Solids, Nöthnitzer Straße 40, D-01187 Dresden, Germany

Received 7 June 2004

Published 16 July 2004

Online at stacks.iop.org/JPhysCM/16/5427

doi:10.1088/0953-8984/16/30/005

Abstract

We have grown single crystals of ThCoGa₄ by the self-flux method. X-ray examination showed that it crystallizes in an orthorhombic structure of the YNiAl₄-type. Electron transport properties examination between 2 and 300 K allowed us to determine its phonon components to the electrical resistivities/thermoelectric powers, which at 300 K are equal (in $\mu\Omega$ cm/ μ V K⁻¹) to 17.3/11.7, 40.6/1.9 and 35.0/2.7, along the *a*-, *b*-, and *c*-axes, respectively. Specific heat examination allowed us to estimate the Sommerfeld coefficient and Debye temperature, which are equal to 6.9 (± 0.3) mJ K⁻² mol⁻¹ and 288 K, respectively. ThCoGa₄ was found to be a paramagnet with a nearly temperature independent susceptibility above 30 K, equal to about 6.7×10^{-5} emu mol⁻¹.

(Some figures in this article are in colour only in the electronic version)

1. Introduction

Guided by the discovery of the new heavy fermion compounds CeTIn₅, where T = Co, Rh, Ir [1, 2], we have tried to grow single crystals of isostructural uranium and thorium compounds with gallium. We have succeeded in growing single crystals of UCoGa₅ and URhGa₅ [3]. They do not show any phase transitions, including superconducting ones, down to 0.4 K, though CeCoIn₅ shows unconventional superconductivity at $T_C = 2.3$ K [2], while CeRhIn₅ is an incommensurate antiferromagnet that transforms to a superconductor with $T_C = 2.1$ K at pressures greater than 1.6 GPa [4].

Two-band conductor behaviour of the electrical resistivity ($\rho(T)$) was observed for URhGa₅ [3] and UCoGa₅ [5, 6], in consistency with a semimetallic-type Fermi surface found for these two uranium compounds [7, 8]. It is interesting that the room temperature

thermoelectric power $S(300\text{ K})$ for these two compounds exceeds $60\ \mu\text{V K}^{-1}$ [3, 6], leading to an enhanced value of the dimensionless figure of merit $ZT = S^2T/\rho\kappa$ (κ : thermal conductivity) close to 0.065 at temperatures between 200 and 300 K for URhGa₅ [3].

Our attempt to grow ThCoGa₅ in exactly the same way as we have grown UCoGa₅ and URhGa₅ resulted in crystals of ThCoGa₄, crystallizing in an orthorhombic structure of YNiAl₄-type. To our best knowledge ThCoGa₄ is the first representative of actinide compounds crystallizing in the YNiAl₄-type structure. Therefore we have examined ThCoGa₄ with the x-ray diffraction method, determined its $\rho(T)$ and $S(T)$ along the three principal crystal axes, the b -axis magnetic susceptibility $\chi(T)$, and the low temperature heat capacity $C_p(T)$.

2. Experimental details

Single crystals of ThCoGa₄ were grown by a self-flux method similar to that used for growing CeRhIn₅ and CeIrIn₅ [1]. Th (of purity 99.9%), Co (of purity 99.99%) and Ga (99.999%) at a ratio 1:1:20 were placed in an alumina crucible, and the crucible was encapsulated in a quartz tube with He under pressure of 200 mm Hg at ambient temperature. The capsule was heated to 1100 °C, was allowed to equilibrate for 2 h and then cooled slowly to 700 °C with the rate increasing from 3 to 10 °C h⁻¹. The hot (700 °C) capsule was rapidly immersed into liquid nitrogen. The ThCoGa₄ crystals were drawn out of the Ga flux, warmed up to 60 °C, and washed carefully with mercury to remove the residual Ga flux. The Hg was removed by distillation in vacuum at 300 °C.

The room temperature x-ray intensity data were collected in an Xcalibur-Oxford-Diffraction four-circle single crystal diffractometer equipped with CCD camera using graphite-monochromatized Mo K α radiation ($\lambda = 0.71073\ \text{\AA}$). The intensities of reflections were corrected for Lorentz and polarization effects. An analytical absorption correction was applied.

The electrical resistivity and the thermoelectric power were investigated in the temperature range 0.35–300 K. The resistivity was measured by a conventional four-point dc method. A method described in [9] was used for the thermoelectric power measurements. To determine the anisotropy of the transport properties, different samples with lengths 2.5, 0.8 and 0.9 mm were cut out from the same single crystal along the a -, b - and c -axes, respectively. The dc magnetic susceptibility in fields applied along the b -axis was measured with a superconducting quantum interference device magnetometer (Quantum Design). The specific heat between 0.4 and 14 K was determined with the aid of the thermal-relaxation technique utilizing a commercial microcalorimeter (Quantum Design).

3. Results

3.1. Crystal structure

The crystal structure of ThCoGa₄ was determined using the x-ray diffraction (XRD) method for a crystal of size $0.02 \times 0.02 \times 0.02\ \text{mm}^3$. As many as 3928 reflections (1015 unique, $R_{\text{int}} = 0.0831$) were recorded to resolve the structure by the direct method [10] and were refined by the full matrix least squares method using the SHELX-97 program [11], with a final discrepancy factor $R = 0.0429$ (for $I > 2\sigma(I)$ $R = 0.0378$). The XRD examination showed that the unit cell of the examined crystal belongs to an orthorhombic system of the YNiAl₄-type structure ($Cmcm$ space group) [12], with 4 fu in the unit cell, whose parameters are $a = 4.161(1)\ \text{\AA}$, $b = 15.682(3)\ \text{\AA}$, $c = 6.570(1)\ \text{\AA}$.

Important crystal structure parameters are collected in tables 1 and 2. The projection of the unit cell along the a -axis with some coordination polyhedra of atoms is shown in figure 1.

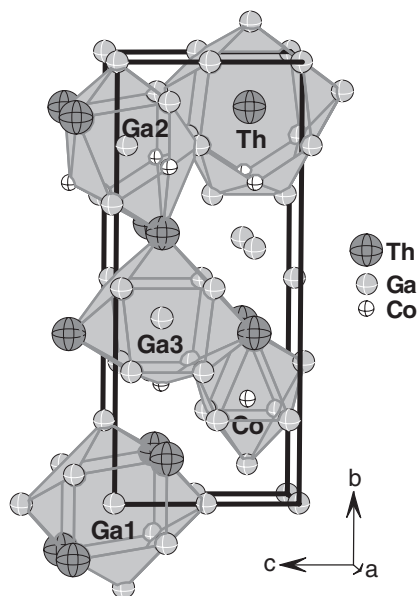


Figure 1. Projection of the unit cell of ThCoGa₄ along the *a*-axis with coordination polyhedra of atoms.

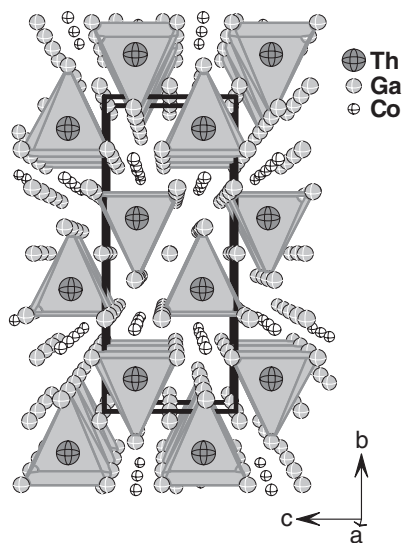


Figure 2. The arrangement of Th[4Ga₂ Ga₃] square pyramids (the first coordination sphere of Th) in ThCoGa₄.

Table 1. Atomic coordinates and anisotropic displacement parameters ($\text{\AA}^2 \times 10^3$) for ThCoGa₄. (Note: $U_{13} = U_{12} = 0$; $U(\text{eq})$ is defined as one third of the trace of the orthogonalized U_{ij} tensor. The anisotropic displacement factor exponent takes the form $-2\pi^2[h^2a^{*2}U_{11} + \dots + 2hka^*b^*U_{12}]$.)

Atom	Site	<i>x</i>	<i>y</i>	<i>z</i>	U_{11}	U_{22}	U_{33}	U_{23}
Th	4c <i>m2m</i>	0	0.3858(1)	1/4	8(1)	8(1)	9(1)	0
Ga1	4a <i>2/m..</i>	0	0	0	11(1)	12(1)	17(1)	4(1)
Ga2	8f <i>m..</i>	0	0.1899(1)	0.0553(1)	9(1)	16(1)	10(1)	-2(1)
Ga3	4c <i>m2m</i>	0	0.5788(1)	1/4	16(1)	12(1)	12(1)	0
Co	4c <i>m2m</i>	0	0.7270(1)	1/4	11(1)	12(1)	13(1)	0

The coordination polyhedron of Th, the atom of largest size, can be considered as a pentagonal prism with five additional atoms; however, the nearest five Ga atoms (the first coordination sphere) create square pyramids oriented up and down along the *b*-axis (see figure 2). All Ga atoms are coordinated by 12 neighbours forming more or less deformed cubo-octahedrons. The coordination polyhedron of Co, the atom of smallest size (tricapped trigonal prism), contains nine atoms.

3.2. Electrical resistivity

The electrical resistivity of ThCoGa₄ along the *a*-, *b*-, and *c*-axes is presented in figure 3. The low-temperature $\rho(T)$ data for ThCoGa₄ resistivity ($T < 36$ K) fit well to the formula $\rho = \rho_0 + AT^n$ with $n = 3$, and $\rho_0 = 21.74, 75.75,$ and $63.57 \mu\Omega \text{ cm}$ and $A = 1.989 \times 10^{-5}, 3.834 \times 10^{-5},$ and $3.594 \times 10^{-5} \mu\Omega \text{ cm K}^{-3}$ for the *a*-, *b*-, and *c*-axes, respectively.

Based on Matthiessen's rule it seems reasonable to assume that ρ_0 is the residual resistivity due to static impurities, while $\rho_{\text{ph}}(T) = \rho(T) - \rho_0$ is the phonon component of the resistivity

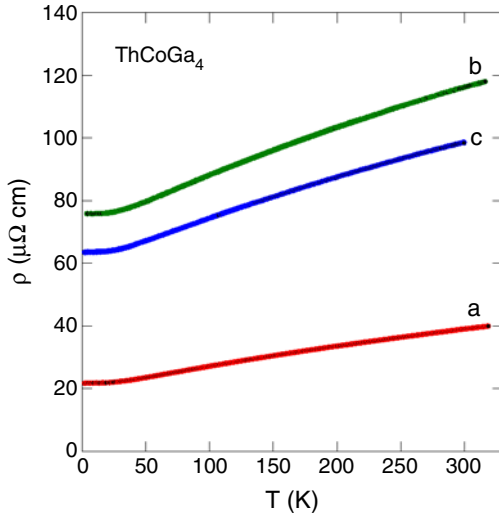


Figure 3. Temperature dependence of the electrical resistivity along the *a*-, *b*-, and *c*-axes of ThCoGa₄.

Table 2. Interatomic distances for ThCoGa₄.

Th:	1 Ga3	3.0261(15)	Ga2:	1 Co	2.3921(12)
CN = 15	4 Ga2	3.1244(7)	CN = 12	2 Co	2.5106(7)
	4 Ga1	3.1986(4)		1 Ga2	2.5585(16)
	2 Co	3.2457(13)		2 Ga2	2.9000(13)
	2 Ga2	3.3284(11)		1 Ga1	3.0000(11)
	2 Ga3	3.3315(5)		2 Ga3	3.0000(11)
Co:	1 Ga3	2.324(2)		2 Th	3.1244(7)
CN = 9	2 Ga2	2.3921(12)		1 Th	3.3284(11)
	4 Ga2	2.5106(7)	Ga3:	1 Co	2.324(2)
	2 Th	3.2457(13)	CN = 12	4 Ga1	2.9247(7)
Ga1:	4 Ga3	2.9247(7)		4 Ga2	3.0000(11)
CN = 12	2 Ga2	3.0000(11)		1 Th	3.0261(15)
	4 Th	3.1986(4)		2 Th	3.3315(5)
	2 Ga1	3.2850(5)			

in the whole temperature range. Values of the latter at 300 K, $\rho_{\text{ph}}(300 \text{ K})$, are 17.28, 40.62, and 35.03 $\mu\Omega \text{ cm}$ for the *a*, *b*, and *c*-axes, respectively. It is worth noticing that for all three crystal axes examined, the ratios $\rho_{\text{ph}}(T)/\rho_{\text{ph}}(300 \text{ K})$ fit to one curve shown in the inset of figure 4. In turn the AT^3 term corresponds to the low temperature limit ($T \ll \Theta_{\text{D}} = \text{Debye temperature}$) of the generalized Bloch–Grüneisen (BG) formula for power $n = 3$ [13, 14, 3]:

$$\rho_{\text{BG}}(T) = C(T/\Theta_{\text{D}}^R)^n \int_0^{\Theta_{\text{D}}^R/T} \frac{z^n dz}{(e^z - 1)(1 - e^{-z})}. \quad (1)$$

This formula, like the original BG formula (for $n = 5$), predicts a linear increase of the resistivity with temperature in the high temperature limit ($T \gg \Theta_{\text{D}}$). The dashed line in figure 4 presents the $\rho_0 + \rho_{\text{BG}}(T)$ sum where the $\rho_{\text{BG}}(T)$ dependence is determined for those parameters obtained for the best fit of the *b*-axis data below 120 K: $C = 30.48 \mu\Omega \text{ cm}$ and $\Theta_{\text{D}}^R = 212 \text{ K}$. At the highest temperatures, however, the experimental data deviate from the predicted linear temperature dependence of the electrical resistivity.

The temperature dependence of the phonon component of the resistivity for ThCoGa₄ resembles that for the nonmagnetic ReMe₃ compounds (Re = La and Lu; Me = Sn, Pb, In,

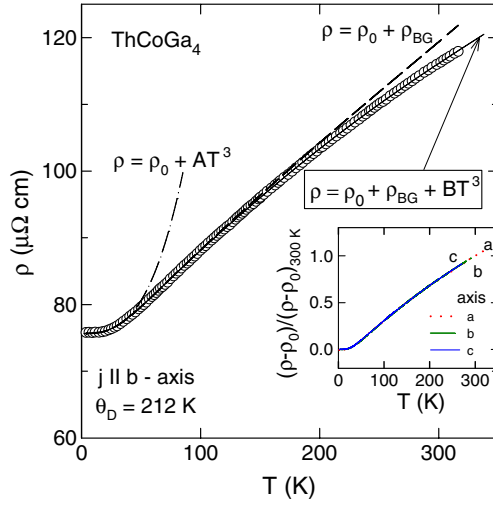


Figure 4. Open circles show the b -axis $\rho(T)$ data for ThCoGa₄; the dash-dotted curve presents the resistivity given by the $\rho_0 + AT^3$ sum fitted to the experimental data below 36 K; the dashed line represents the resistivity given by the sum of the generalized Bloch–Grüneisen formula (equation (1)) and the residual resistivity, $\rho(T)_{BG} + \rho_0$; the latter completed by a negative BT^3 term is shown by the solid curve. Details are given in the text. The inset shows that the normalized phonon resistivities $\rho_{ph}(T)/\rho_{ph}(300 \text{ K})$ fall on top of each other for the three main crystal axes.

and Ga) [14] and for URhGa₅ [3] as well. At high temperatures, nonlinear $\rho(T)$ dependences in connection with relatively large absolute values (e.g. for LaPb₃, $\rho(300 \text{ K}) = 34 \mu\Omega \text{ cm}$) have been ascribed to s - d -type scattering in two-band metals. According to Mott's theory [15], s - d scattering leads to an additional, high temperature BT^3 term in the electrical resistivity. Both the value of B and its sign depend on the density of d states at the Fermi level, $N_d(E_F)$. Taking into account the overall similarity in $\rho(T)$ between ReMe₃ and ThCoGa₄, we used the Mott approach to the latter one as well. The deviation of the data from the $\rho(T)_{BG}$ term above $T = 120 \text{ K}$ can be accounted for by a BT^3 term with $B = -1.24 \times 10^{-7} \mu\Omega \text{ cm K}^{-3}$; see figure 4 (solid curve). This value can be compared to values of B equal to $-1.2 \times 10^{-7} \mu\Omega \text{ cm K}^{-3}$ for LaPb₃ [14] to $-1.23 \times 10^{-6} \mu\Omega \text{ cm K}^{-3}$ for URhGa₅ and to $-(1.5\text{--}4.6) \times 10^{-6} \mu\Omega \text{ cm K}^{-3}$ for R₆Me₂₃ (R = Y, Er and Me = Mn, Fe) [16].

3.3. Thermoelectric power

In figure 5 the thermoelectric power data are shown as a function of temperature for the three main crystal axes of ThCoGa₄. $S(T)$ is very anisotropic and positive in the whole temperature range examined. The anisotropy can be characterized by $S(300 \text{ K})$ values equal to 11.7, 1.9 and $2.7 \mu\text{V K}^{-1}$ for the a -, b -, and c -axes, respectively. The inset in figure 5 displays the low temperature part of the $S(T)$ behaviour for both the b - and c -axes, revealing a peak at about 17 K.

The low temperature part of the c -axis thermoelectric power can be approximated by a formula $S(T) = AT + BT^3$, where the A coefficient is ${}^L A_c = 0.0338 \mu\text{V K}^{-2}$ and $B = 0.000648 \mu\text{V K}^{-4}$. In general, the b - and c -axis $S(T)$ behaviour can be understood as the sum of two components: linear in temperature and the peak-like one. Such behaviour is observed for the case when the thermoelectric power is composed of the diffusion thermoelectric power

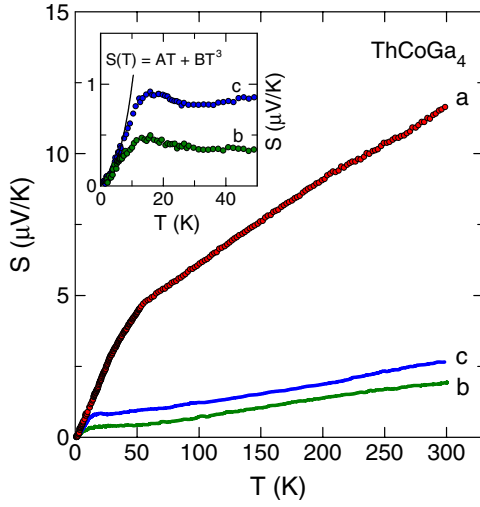


Figure 5. Temperature dependence of the thermoelectric power along the a -, b -, and c -axes for ThCoGa_4 . The inset shows the low- T data for the b - and c -axes; the solid curve represents equation (2): $S(T) = AT + BT^3$ fitted to the c -axis data.

S_d on the one hand and the phonon-drag one S_g on the other:

$$S(T) = S_d(T) + S_g(T). \quad (2)$$

Usually at a temperature $\sim(0.1-0.3)\Theta_D^R$, the $S_g(T)$ thermoelectric power has a maximum and depends on temperature as $\sim T^3$ well below and as $1/T$ well above the maximum, respectively [17]. Assuming $S_g(300 \text{ K}) = 0$, this approach applied to the a -axis $S(T)$ allows one to decompose it into two components, one being linear in temperature and the other one of a peak shape. The maximum of this latter component is observed at $T \approx 55 \text{ K}$, and this fits to the temperature range where it is expected for the $S_g(T)$ component. However, the temperature dependence of the a -axis peak-like $S_g(T)$ component differs substantially from the above-mentioned standard behaviour, both below and above the peak temperature.

The diffusion term $S_d(T)$ is described by the well-known Mott formula:

$$S_d(T) = AT; \quad A = \xi(\pi^2 k^2)/3eE_F, \quad (3)$$

where k and e are the Boltzmann constant and electron charge, respectively, while E_F is the Fermi energy. The thermoelectric parameter ξ depends on the mechanism of the electron scattering and may vary between 1 and 3 [18]. Assuming $S_g(300 \text{ K}) = 0$ we can determine the A coefficient for the high temperature range denoted by $^H A_a$, $^H A_b$, and $^H A_c$ for the a -, b -, and c -axes, respectively. They are equal to 0.0389, 0.0064, and 0.0089 $\mu\text{V K}^{-2}$, respectively. Surprisingly enough, $^L A_c = 0.0338 \mu\text{V K}^{-2}$ is found to be much closer to $^H A_a$ than to $^H A_c$. Taking $\xi = 2$ and $^H A_a = 0.0389 \mu\text{V K}^{-2}$ one can, within the one-band approximation, roughly estimate the Fermi energy: $E_F \approx 2 \text{ eV}$. Of course, assuming a single isotropic band is not sufficient in view of the observed thermoelectric power anisotropy.

3.4. Thermodynamic properties

The specific heat $C(T)$ examination of ThCoGa_4 has not shown any phase transition, including a superconducting one, between 0.4 and 14 K. The $C(T)$ data are shown in a log-log plot in figure 6. The inset displays C/T versus T^2 . From the straight line found for $T \approx 4 \text{ K}$ one obtains the Sommerfeld coefficient $\gamma = 6.9(\pm 0.3) \text{ mJ K}^{-2} \text{ mol}^{-1}$ and the slope $\beta = 0.488 \times 10^{-3} \text{ J K}^{-4} \text{ mol}^{-1}$, which yields a Debye temperature $\Theta_D = 288 \text{ K}$ ($\beta = 6 \times 1944/\Theta_D^3$).

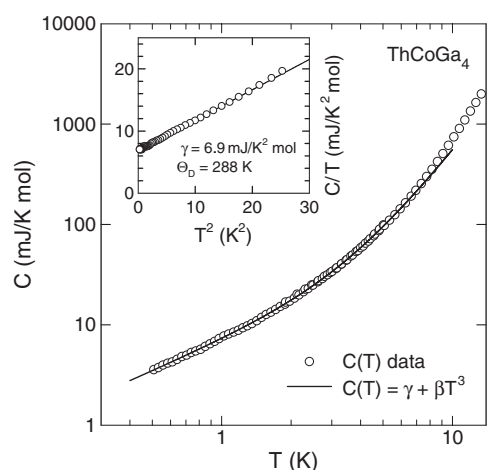


Figure 6. The low temperature specific heat of a ThCoGa₄ single crystal shown in a double-logarithmic plot. The solid curve represents a $\gamma T + \beta T^3$ dependence. The inset displays the low- T specific heat, as $C(T)/T$ versus T^2 .

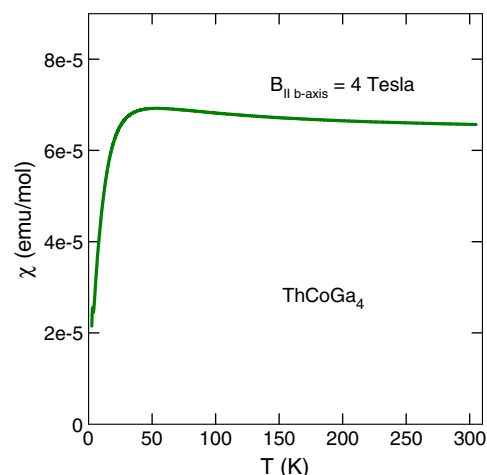


Figure 7. Temperature dependence of the magnetic susceptibility of a ThCoGa₄ single crystal in magnetic field of 4 T.

The magnetic susceptibility $\chi(T)$ of ThCoGa₄ (figure 7) was measured in a magnetic field 4 T applied parallel to b -axis in the temperature range 1.7–300 K. All ThCoGa₄ crystals are paramagnetic. After an initial sharp increase, the $\chi(T)$ passes through a flat maximum at $T \approx 54$ K, where it reaches a value of approximately 7.0×10^{-5} emu mol⁻¹. The $\chi(T)$ behaviour above 50 K represents typical metallic paramagnetism of the Pauli type.

4. Discussion and conclusions

Orthorhombic ThCoGa₄ shows considerable anisotropy of its electrical resistivity. The resistivity along the a -axis is apparently lower than that along both the b - and c -axes. It is interesting that the projection of the crystal along the a -axis, shown in figure 2, looks very transparent due to the linear arrangement of the atoms composing this crystal. Assuming the validity of Matthiessen's rule, the resistivity was resolved into a temperature independent part electron scattering from static defects—residual resistivity—and the remaining part. The latter was analysed in terms of the generalized Bloch–Grüneisen formula for power $n = 3$ [13, 14, 3] and ascribed to the phonon contribution to the resistivity.

The residual resistivities of the examined samples along the b - and c -axes are larger by a factor of 3.5 and 2.9 than that for the a -axis, respectively. Though these factors differ from the corresponding factors for $\rho_{\text{ph}}(300 \text{ K})$, 2.3 and 2.0, they all highlight substantial anisotropy in the resistivity behaviour.

It is evident from the inset of figure 4 that the ratios of the total resistivities along the a - b - and c -axes composed of the components of the two different scattering mechanisms is temperature dependent, while the corresponding ratios for $\rho_{\text{ph}}(T)$ are temperature independent within the accuracy of the experiment. This latter behaviour is the most natural, since $\rho_{\text{ph}}(T)$ represents one single mechanism of electron scattering in the whole temperature range, namely the scattering of electrons by phonons. At high temperatures this electron–phonon scattering in a *two-band* metal may lead to a significant deviation of the measured $\rho_{\text{ph}}(T)$ from the linear temperature dependence. Such a deviation should be anisotropic in $\mu\Omega \text{ cm}$ units and

isotropic in terms of the normalized resistivity $\rho_{\text{ph}}(T)/\rho_{\text{ph}}(300 \text{ K})$, in good agreement with our observations.

Stoichiometric ThCoGa₄ has an even number of valence electrons per unit cell, hence per Brillouin zone. Thus ThCoGa₄ should be a compensated metal or semimetal, i.e. it should have equal numbers of holes and electrons. In such a case cancellation of electron and hole parts may play an important role for the thermoelectric effects, unless there is a considerable difference between the electrons' and holes' mobilities; the contribution of a particular band to the total thermoelectric power is weighted by the ratio of the particular band's conductivity to the total conductivity. For these reasons the low values of the thermoelectric power for ThCoGa₄ observed both along the *b*- and the *c*-axes may be ascribed to a considerable cancellation effect. The latter appears to be greatly reduced for the *a*-axis thermoelectric power due to a considerable increase of the holes' mobility along the *a*-axis, as manifested by the low $\rho_{\text{ph}}(T)$ -values measured along the *a*-axis. Such an interpretation allows us to assume that the hole band dominates the *a*-axis thermoelectric power and the single-band approximation can be applied for a rough estimation of the Fermi energy for this band. The relatively low value $E_{\text{F}} \approx 2 \text{ eV}$ that we obtain is consistent with transition-metal-like $\rho_{\text{ph}}(T)$ dependence.

In conclusion, ThCoGa₄ grown by the self-flux method crystallizes in an orthorhombic structure of the YNiAl₄-type. It is an anisotropic metal with values of both the resistivity and the thermoelectric power being similar to those commonly observed for transition metals. Consistent with this behaviour are a Pauli-type paramagnetism with a susceptibility value of $7.0 \times 10^{-5} \text{ emu mol}^{-1}$ and a Sommerfeld coefficient of the electronic specific heat $\gamma = 6.9 \text{ mJ K}^{-2} \text{ mol}^{-1}$.

Acknowledgment

We thank MSc R Gorzelniak for his help during the magnetic susceptibility measurements.

References

- [1] Moshopoulou E G, Fisk Z, Sarrao J L and Thomson J D 2001 *J. Solid State Chem.* **158** 25
- [2] Petrovic C, Pagliso P G, Hundley M F, Movshovich R, Sarrao J L, Thomson J D, Fisk Z and Montoux P 2001 *J. Phys.: Condens. Matter* **13** L337
- [3] Wawryk R, Henkie Z, Cichorek T, Geibel C and Steglich F 2002 *Phys. Status Solidi b* **232** R4
- [4] Hegger H, Petrovic C, Moshopoulou E G, Hundley M F, Sarrao J L, Fisk Z and Thomson J D 2000 *Phys. Rev. Lett.* **84** 4986
- [5] Morkowski J, Szajek A, Bukowski Z, Sułkowski C, Troć R and Chełkowska G 2004 *J. Magn. Magn. Mater.* **272–6** e223–4
- [6] Troć R, Bukowski Z, Sułkowski C, Misiorek H, Morkowski J, Szajek A and Chełkowska G 2004 *Phys. Rev. B* at press
- [7] Ikeda S, Tokiwa Y, Okubo T, Haga Y, Yamamoto E, Inada Y, Settai R and Onuki Y 2002 *J. Nucl. Sci. Technol.* **3** (Suppl.) 206
- [8] Ikeda S *et al* 2003 *Physica B* **329–333** 610
- [9] Wawryk R and Henkie Z 2001 *Phil. Mag.* **B 81** 223–4
- [10] Sheldrick G M 1985 *Program for the Solution of Crystal Structures* (Germany: University of Göttingen)
- [11] Sheldrick G M 1987 *Program for Crystal Structure Refinement* (Germany: University of Göttingen)
- [12] Rykhal' R M, Zarechnyuk O S and Yarmolyuk P Ya 1971 *Sov. Phys.—Crystallogr.* **17** 454–5
- [13] Grimvall G 1986 *Thermophysical Properties of Materials* (Amsterdam: North-Holland) p 218
- [14] Kletowski Z, Fabrowski R, Sławiński P and Henkie Z 1997 *J. Magn. Magn. Mater.* **166** 361
- [15] Mott N F 1936 *Proc. R. Soc.* **156** 368
- [16] Gratz E and Kirchmayr H R 1976 *J. Magn. Magn. Mater.* **2** 187
- [17] Blatt F J, Schroeder P A, Foiles C L and Greig D 1976 *Thermoelectric Power of Metals* (New York: Plenum) pp 91–2
- [18] Barnard R D 1972 *Thermoelectricity in Metals and Alloys* (London: Taylor and Francis) p 58